

# [70]Fullerene-Based Materials for Organic Solar Cells

Pavel A. Troshin,<sup>\*[a]</sup> Harald Hoppe,<sup>[b]</sup> Alexander S. Peregudov,<sup>[c]</sup> Martin Egginger,<sup>[d]</sup> Sviatoslav Shokhovets,<sup>[b]</sup> Gerhard Gobsch,<sup>[b]</sup> N. Serdar Sariciftci,<sup>[d]</sup> and Vladimir F. Razumov<sup>[a]</sup>

The synthesis, characterization and photovoltaic study of two novel derivatives of [70]fullerene, phenyl-C<sub>71</sub>-propionic acid propyl ester ([70]PCPP) and phenyl-C<sub>71</sub>-propionic acid butyl ester ([70]PCPB), are reported. [70]PCPP and [70]PCPB outperform the conventional material (6,6)-phenyl-C<sub>71</sub>-butyric acid methyl ester ([70]PCBM) in solar cells based on poly(2-methoxy-5-{3',7'-dimethyloctyloxy}-*p*-phenylene vinylene) (MDMO-PPV) as a donor polymer using chlorobenzene (CB) or dichlorobenzene (DCB) as solvents. AFM data suggest that improvement of the device efficiency should be attributed to the increased phase compatibility between the novel C<sub>70</sub> derivatives and the polymer matrix. [70]PCPP and [70]PCBM showed more

or less equally high performances in solar cells comprising poly(3-hexylthiophene) (P3HT) as a donor polymer. Optical modeling revealed that the application of [70]fullerene derivatives as acceptor materials in P3HT-based bulk heterojunction solar cells might give approximately 10% higher short circuit current densities than using C<sub>60</sub>-based materials such as [60]PCBM. The high solubility of [70]PCPP and [70]PCPB and their good compatibility with the donor polymers suggest these fullerene derivatives as promising electron acceptor materials for use in efficient bulk heterojunction organic solar cells.

## Introduction

Intensive worldwide research in the field of organic solar cells has resulted in the development of novel highly efficient material combinations and laboratory-scale devices with certified power conversion efficiencies of 6–7%.<sup>[1–3]</sup> Highly efficient solution-based technologies applied to the fullerene/polymer blends should allow for industrial production of cheap organic solar cell modules.<sup>[4–6]</sup> The feasibility of this approach was demonstrated by Konarka Technologies, who launched the first production facility in the USA in 2009.<sup>[7]</sup> Recent estimations suggest that electricity generation at the cost of 5–10 cents per kWh is quite achievable using organic solar batteries.<sup>[8]</sup>

Intensive research during last few years was focused almost entirely on the design of novel low band-gap conjugated polymers.<sup>[9–11]</sup> However, few reports clearly demonstrated that fullerene component also has to be optimized to reach maximal performance.<sup>[12–20]</sup> A recent review addressed the structural design of fullerene-based acceptor materials for organic solar cells.<sup>[21]</sup> Another important issue is that almost all known low band-gap polymers yield high power conversion efficiencies in solar cells only when combined with (6,6)-phenyl-C<sub>71</sub>-butyric acid methyl ester ([70]PCBM).<sup>[2,3,22–26]</sup> Fortunately, the cost of pristine C<sub>70</sub> has decreased in recent years and is now 300–500 USD g<sup>-1</sup>.<sup>[27]</sup> Taking into account the low thickness of the light-harvesting layer in organic solar cells (100–200 nm), the cost of the materials, if they remain as expensive as [70]fullerene derivatives, should not be a crucial issue for their successful commercialization.

Surprisingly, the range of alternative [70]fullerene derivatives used in organic solar cells is very limited. To our knowledge, only BTPF70<sup>[28,29]</sup> and some C<sub>70</sub>-based fullerene dimers<sup>[30]</sup> be-

side [70]PCBM were applied in organic photovoltaics.<sup>[31]</sup> We recently demonstrated that the physical properties and, in particular, solubility of the fullerene-based component has a strong influence on the performance of polymer–fullerene solar cells.<sup>[16,17]</sup> In particular, fullerene derivative with matching solubility should be provided for every novel low band gap polymer to give maximal photovoltaic performance of the blend. Therefore, a family of [70]fullerene derivatives with variable solubilities and other physical properties should be designed and applied in studies of novel low band-gap copolymers.

Herein we report preparation and investigation of two novel [70]fullerene derivatives, phenyl-C<sub>71</sub>-propionic acid propyl ester ([70]PCPP) and phenyl-C<sub>71</sub>-propionic acid butyl ester ([70]PCPB), following the nomenclature introduced by Humme-

[a] P. A. Troshin, V. F. Razumov

*Institute of Problems of Chemical Physics of Russian Academy of Sciences  
Semenov Prospect 1, Chernogolovka, Moscow region, 142432 (Russia)*

*Fax: (+7) 496-522-3507*

*E-mail: troshin2003@inbox.ru*

[b] H. Hoppe, S. Shokhovets, G. Gobsch

*Ilmenau University of Technology, Institute of Physics  
Weimarer Str. 32, 98693 Ilmenau (Germany)*

[c] A. S. Peregudov

*A. N. Nesmeyanov Institute of Organoelement Compounds  
1 Vavilova St. 28, B-334, Moscow, 119991 (Russia)*

[d] M. Egginger, N. S. Sariciftci

*Linz Institute for Organic Solar Cells (LIOS), Johannes Kepler University Linz  
Altenbergerstrasse 69, 4040 Linz (Austria)*



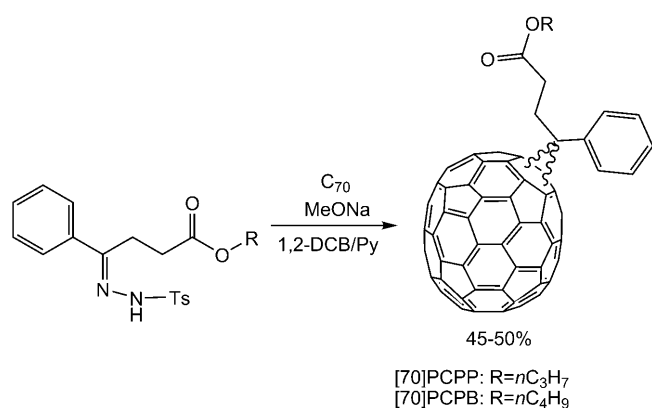
Supporting information for this article is available on the WWW under <http://dx.doi.org/10.1002/cssc.201000246>.

len et al. for [70]PCBM.<sup>[31]</sup> The designed compounds incorporate longer alkyl groups at the ester functionality (propyl and butyl instead of methyl in PCBM), which should improve the compatibility of these fullerene derivatives with conjugated polymers that are decorated with long solubilizing alkyl side chains. Owing to such structural modifications, [70]PCPP and [70]PCPB might be considered as promising acceptor materials for investigation in polymer–fullerene bulk heterojunction solar cells.

## Results and Discussion

### Synthesis

Both [70]PCPP and [70]PCPB were synthesized using a modified Hummelen–Wudl procedure, first applied for the synthesis of [60]PCBM and [70]PCBM (Scheme 1).<sup>[32]</sup> Benzoylpropionic



**Scheme 1.** Synthesis of [70]PCPP and [70]PCPB.

acid was used as a precursor due to its much lower price and higher availability in comparison with the benzoylbutyric acid used for preparation of PCBM. Derivatives of [70]fullerene were obtained as typical mixtures of 3 isomers where content of the major 1,2-addition product (8,25 according to new IUPAC nomenclature) was in the range of 83–88%. Careful column chromatography on silica with toluene/hexane eluent allowed isolation of [70]PCBM, [70]PCPP, and [70]PCPB with isomeric purities as high as 90–95%. These values were supported by <sup>1</sup>H NMR spectroscopy and HPLC. Molecular structures of the new compounds were also confirmed by <sup>13</sup>C NMR spectroscopy, absorption spectroscopy (absorption features of 1,2-addition product are quite characteristic) and chemical analysis.

### Solar cells with MDMO-PPV

Poly(2-methoxy-5-[3',7'-dimethyloctyloxy]-*p*-phenylene vinylene) (MDMO-PPV; Figure 1) was one of the first conjugated polymers successfully applied as an electron-donor material for fabrication of bulk heterojunction solar cells. The photovoltaic potential of MDMO-PPV is very limited due to its narrow absorption spectrum, which allows collection of only a small frac-

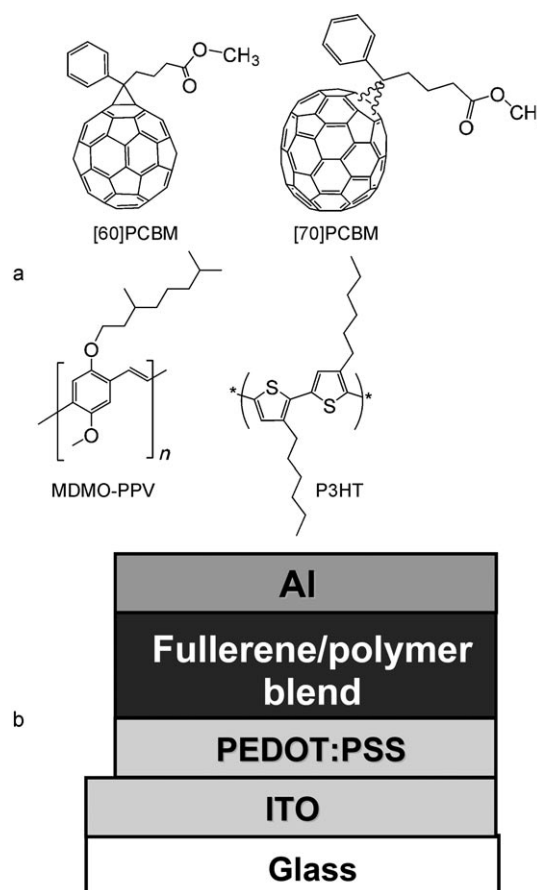


**Figure 1.** a) Molecular structures of the commercially available materials used in this work; b) schematic layout of organic bulk heterojunction solar cell.

tion of the solar irradiation. Nevertheless, MDMO-PPV has been investigated in great detail as a model system. Most importantly, the advantages of [70]fullerene derivatives over the respective [60]fullerene analogues were first demonstrated in solar cells using MDMO-PPV as a donor polymer.<sup>[31]</sup>

We fabricated photovoltaic cells using MDMO-PPV as polymer component combined with one of the C<sub>70</sub> derivatives, [70]PCPP or [70]PCPB, or with the reference compound [70]PCBM (Table 1). Photoactive fullerene derivative/MDMO-PPV blends were casted from chlorobenzene (CB) or from 1,2-dichlorobenzene (DCB) solvents. The power conversion efficiencies of organic solar cells fabricated using DCB as a solvent were significantly higher than those of the cells processed with CB. This solvent effect was reported previously for [70]PCBM/MDMO-PPV blends.

For both CB-cast and DCB-cast cells, power conversion efficiency increases in the order [70]PCBM < [70]PCPP ≤ [70]PCPB. This is particularly illustrated by the *I*-*V* curves for the devices produced using DCB as solvent (Figure 2).

To explain these results, we investigated the topology of the fullerene derivative/polymer blends by atomic force microscopy (AFM; Figure 3). First we studied a series of the films deposited from CB (Figure 3, left column). [70]PCBM/MDMO-PPV blend gave very inhomogeneous films due to a large-scale

Table 1. Power conversion efficiencies of photovoltaic cells based on different [70]fullerene derivatives and MDMO-PPV.				
Blend	$V_{oc}$ [V]	$I_{sc}$ [ $\text{mA cm}^{-2}$ ]	FF	$\eta$ [%]
Cast from chlorobenzene				
[60]PCBM/MDMO-PPV (4:1 w/w)	0.8	4.4	0.56	2.0
[70]PCBM/MDMO-PPV (5:1 w/w)	0.8	1.3	0.53	0.5
[70]PCPP/MDMO-PPV (5:1 w/w)	0.8	3.0	0.44	1.0
[70]PCPB/MDMO-PPV (5:1 w/w)	0.78	3.8	0.46	1.4
Cast from 1,2-dichlorobenzene				
[70]PCBM/MDMO-PPV (5:1 w/w)	0.74	5.5	0.53	2.2
[70]PCPP/MDMO-PPV (5:1 w/w)	0.8	7.1	0.52	2.8
[70]PCPB/MDMO-PPV (5:1 w/w)	0.8	7.6	0.5	3.1

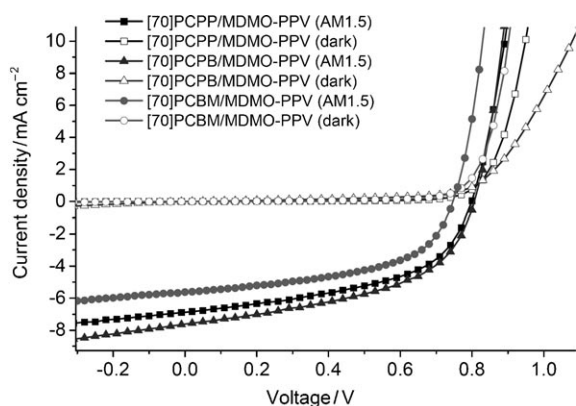


Figure 2. Dark and light-on (AM 1.5,  $100 \text{ mW cm}^{-2}$ )  $I/V$  curves of solar cells comprising MDMO-PPV and different [70]fullerene derivatives processed from 1,2-dichlorobenzene solutions.

phase separation. This results in the appearance of large islands in the polymer matrix presumably corresponding to the clusters of pure fullerene derivative or fullerene-rich domains. These islands are represented by bright, grain-like features in Figure 2. The size of these islands became dramatically reduced when [70]PCBM was replaced with [70]PCPP and then even further reduced when [70]PCPB was used (Figure 3). All blends cast from DCB were much smoother than the CB-processed systems. Nevertheless, [70]PCBM/MDMO-PPV blend showed grainy topology, suggesting significant phase separation in the blend. However, any detectable phase segregation disappears when [70]PCBM is replaced with [70]PCPP and [70]PCPB (Figure 3).

These results suggest that there is clear correlation between the scale of the phase separation in the blends and the photovoltaic performance of these blends. To visualize this effect, we estimated average size of the clusters (grains) in the AFM images of all composites. Afterwards, we plotted short-circuit current density ( $I_{sc}$ ) and power conversion efficiency ( $\eta$ ) of the solar cells against the size of the clusters (grains) determined from the AFM images (Figure 4).

Indeed, both photovoltaic parameters monotonously decrease with increase in the cluster size, which is a good illustration of the morphology control over the device performance

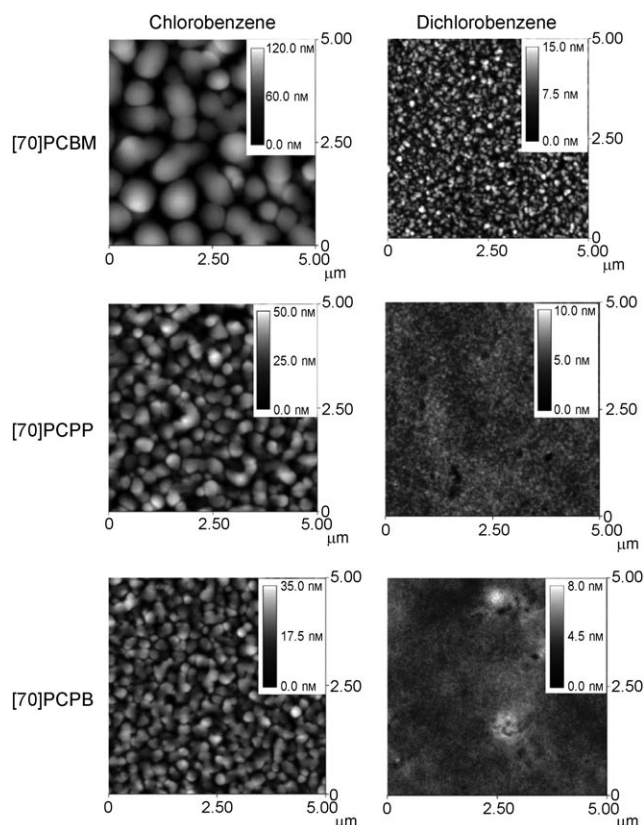


Figure 3. AFM images of the [70]fullerene derivative/MDMO-PPV blend films processed from CB (left column) and DCB (right column).

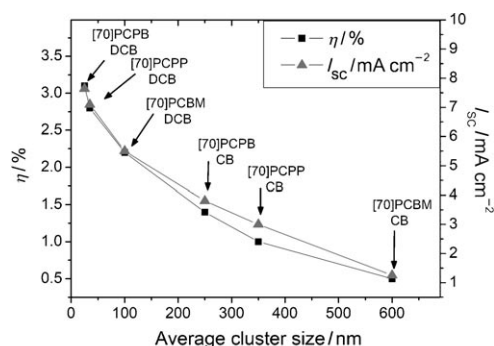


Figure 4. Dependence of the short-circuit current density ( $I_{sc}$ ) and power conversion efficiency ( $\eta$ ) of the solar cells on the size of the clusters (grains) determined from the AFM images.

in MDMO-PPV-based solar cells. The influence of the cluster size on the performance of the MDMO-PPV/PCBM blends in organic solar cells and underlying physical processes have been considered in great detail recently.<sup>[32]</sup> Figure 4 shows that [70]PCPP and [70]PCPB perform better than the reference [70]PCBM due to the improved compatibility of these fullerene derivatives with MDMO-PPV. We believe that such compatibility comes from longer alkyl substituents at the carboxyl group (propyl and butyl) in [70]PCPP and [70]PCPB molecules capable of favorable intermolecular interactions with the polymer side

chains. Thus, we may conclude that derivatives of [70]fullerene designed in this work might be considered as promising electron-acceptor materials for bulk heterojunction organic solar cells.

### Solar cells with poly(3-hexylthiophene)

Poly(3-hexylthiophene) (P3HT) is another model conjugated polymer that has been well studied and is widely used in the ongoing research in the field of organic photovoltaics. Therefore, we investigated [70]PCPP, [70]PCPB, and reference compounds [70]PCBM and [60]PCBM as electron-acceptor materials in combination with P3HT used as the electron-donor component (Table 2).

Blend	$V_{oc}$ [V]	$I_{sc}$ [ $\text{mA cm}^{-2}$ ]	FF	$\eta$ [%]
[60]PCBM/P3HT (7:12 w/w)	0.62	9.8	0.59	3.6
[70]PCBM/P3HT (2:3 w/w)	0.62	11.5	0.56	4.0
[70]PCPP/P3HT (2:3 w/w)	0.66	11.1	0.49	3.6
[70]PCPB/P3HT (2:3 w/w)	0.60	7.9	0.37	1.8

[70]PCPP gives comparably high performances with the references [60]PCBM and [70]PCBM (Table 2). In contrast, solar cells comprising [70]PCPB/P3HT blends yielded much lower power-conversion efficiency. The reason for such behavior might be in the active layer morphology. Indeed, AFM images revealed that [70]PCPB/P3HT composite films are very smooth without any detectable characteristic features suggesting phase separation (Figure 5). Therefore we may assume that [70]PCPB is fairly well mixable with P3HT. This mixability results in a low degree of phase separation and thereby bad percolation. Therefore, photogenerated charge carriers in the [70]PCPB/P3HT blend cannot be transported efficiently to the electrodes and recombine instead. Similar conclusions have been reported for a family of diphenylmethanofullerenes applied as electron acceptors in organic solar cells.<sup>[33,34]</sup> [70]PCPP/P3HT and [70]PCBM/P3HT blends have coarser film topology providing optimal phase separation required for efficient photovoltaic operation (Table 2).

### Optical modeling for solar cells based on [70]PCBM/P3HT blends

For optical modeling of the polymer–fullerene bulk heterojunctions, the complex refractive indices of all device layers were determined and the transfer matrix formalism was applied for describing the coherent light propagation within the photovoltaic device.<sup>[35,36,37]</sup> The refractive indices of [60]PCBM and [70]PCBM blended with P3HT were determined by ellipsometry. From the refractive index, the absorption coefficient is readily calculated; Figure 6 shows a comparison of the two material combinations. Clearly, the absorption coefficient of the

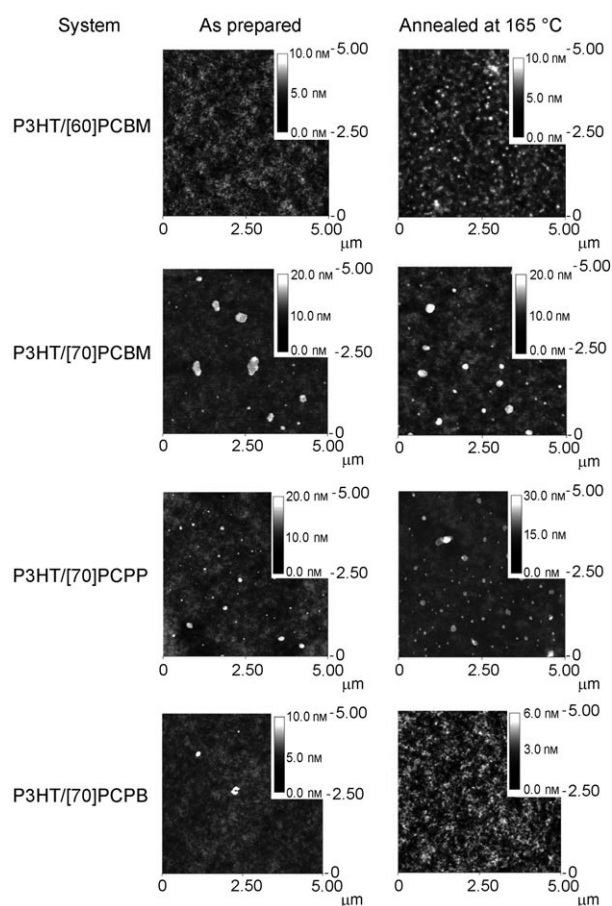


**Figure 5.** AFM images of the fullerene derivative/P3HT blend films as cast (left column) and after thermal annealing at 165 °C for 5 min (right column).

[70]PCBM-based blend is higher within the visible region than that of the [60]PCBM-based blend.

Moreover, as a result of higher absorption coefficient, the calculated absorbed fraction of the incident light is increased for the blend comprising [70]PCBM over the entire visible spectrum (Figure 7). Consequently a higher short-circuit photocurrent is calculated for the [70]PCBM-based blend by folding the absorbed light fraction with the standard AM 1.5 solar irradiation spectrum, which is in agreement with the experimental

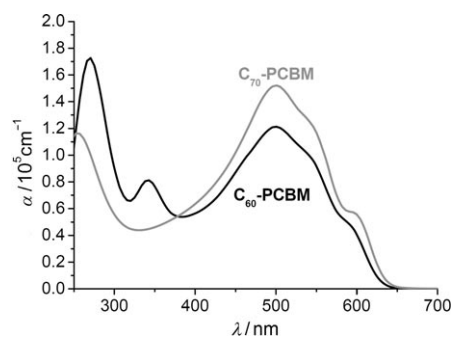


**Figure 6.** Comparison of the absorption coefficients of [70]PCBM and [60]PCBM-based P3HT blends as used as active layer in the photovoltaic devices.

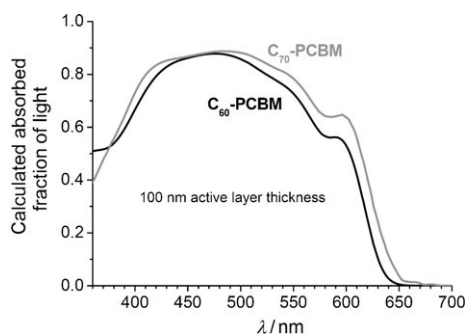


**Figure 7.** Calculated absorbed fractions of the incident light within the photoactive layer of photovoltaic devices based on [70]PCBM and [60]PCBM in combination with P3HT. The [70]PCBM-based blend shows an improved absorption behavior over the [60]PCBM for an active layer thickness of 100 nm.

data shown above. Figure 8 displays the result of the calculation of maximum short-circuit currents—assuming an internal quantum efficiency of unity—for both blends discussed for a wide range of active layer thicknesses. From 70 nm layer thickness there is a significant and almost constant offset to higher densities of short-circuit photocurrent for the [70]PCBM/P3HT blend comparing to [60]PCBM/P3HT system. Both current–active layer thickness relations follow the typical wavy trend arising from interference effects reported previously.<sup>[35,37]</sup>

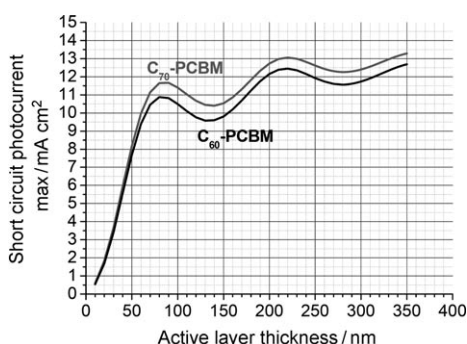


**Figure 8.** Calculated short-circuit photocurrent for [60]PCBM- and [70]PCBM-based bulk heterojunctions with P3HT as the donor polymer for various active layer thicknesses, under the assumption of an internal quantum efficiency of unity. For thicknesses of 70 nm and greater, the [70]PCBM-based photoactive layer produces 0.5–1 mA cm<sup>-2</sup> higher short-circuit current densities than [60]PCBM/P3HT.

## Conclusions

We have verified experimentally and by modeling that C<sub>70</sub> derivatives used as electron-acceptor materials in polymer–fullerene bulk-heterojunction solar cells yield increased photocurrents due to an improved combined absorption strength, when compared to [60]PCBM-based composites.

We have presented two novel highly soluble derivatives of [70]fullerene investigated in model photovoltaic systems using MDMO-PPV and P3HT as donor polymers. It was revealed that [70]PCPP and [70]PCPB, due to peculiarities of their molecular structures, have better phase compatibility with the investigated donor polymers. This effect resulted in a strong improve-

ment of the blend morphology and photovoltaic performance of the MDMO-PPV-based systems. Moreover, P3HT-based devices also exhibited reasonably good performances. On the basis of the experimental data and optical modeling results, the designed compounds [70]PCPP and [70]PCPB might be recommended as improved C<sub>70</sub>-based materials in the study of novel low-band-gap conjugated polymers.

## Experimental Section

### Materials

Polymers MDMO-PPV and P3HT were products of Covion and Rieke Metals companies, respectively. [60]PCBM was purchased from Nano-C company. [70]PCBM was prepared according to the method described in literature.<sup>[31]</sup> All water-free solvents (chlorobenzene, 1,2-dichlorobenzene) were purchased from Aldrich and used as received.

Methanofullerenes [70]PCPP and [70]PCPB were prepared from C<sub>70</sub> and corresponding tosylhydrazones in complete accordance to the method reported previously for the preparation of [70]PCBM.<sup>[31]</sup> The contents of the major 1,2-isomers were determined from the <sup>1</sup>H NMR spectroscopy and HPLC measurements as 90–95%, which is higher than for [70]PCBM; the remaining 5–10% corresponded to two possible diastereoisomers of the minor 5,6-adduct. The obtained [70]PCPP and [70]PCPB isomer mixtures were subjected to spectroscopic characterization and investigation in organic solar cells without further purification.

[70]PCPP (45%): <sup>1</sup>H NMR (CS<sub>2</sub>/(CD<sub>3</sub>)<sub>2</sub>CO 9:1, 400 MHz): δ = 0.88 (t, 0.3H), 1.00 (t, 3H), 1.52 (q, 0.2H), 1.67 (q, 2H), 2.39 (m, 0.4H), 2.73 (m, 4H), 3.77 (t, 0.2H), 4.00 (t, 2H), 7.44 (t, 1.1H), 7.52 (t, 2.2H), 7.79 (d, 0.1H), 7.91 ppm (br d, 2H); <sup>13</sup>C NMR (CS<sub>2</sub>/(CD<sub>3</sub>)<sub>2</sub>CO 9:1, 150 MHz): δ = 11.01(CH<sub>3</sub>), 22.71, 29.81, 30.26, 30.98, 35.19 (methane bridge C), 66.06 (OCH<sub>2</sub>), 69.70 (cage sp<sup>3</sup> C), 71.75 (cage sp<sup>3</sup> C), 128.33, 128.43, 128.72, 129.05, 130.44, 130.63, 130.71, 130.85, 131.62, 132.73, 133.73, 133.92, 136.65, 137.67, 138.61, 139.38, 140.22, 141.05, 141.29, 141.55, 141.77, 142.54, 142.66, 143.27, 143.34, 143.63, 143.70, 143.87, 143.89, 144.08, 144.52, 144.54, 145.48, 145.65, 145.82, 145.91, 146.03, 146.24, 146.78, 146.92, 147.31, 147.38, 147.41, 147.46, 147.65, 147.82, 148.08, 148.28, 148.34, 148.42, 148.46, 148.49, 148.56, 149.03, 149.07, 149.15, 149.28, 149.34, 150.42, 150.47, 150.72, 150.74, 170.74 ppm (COO); MALDI TOF MS: *m/z* = 1044.10 (calculated *m/z* = 1044.11); UV/Vis (toluene): λ = 324, 357, 372, 402, 464, 537 nm; FTIR (KBr): ν = 459 (w), 534 (m), 546 (w), 578 (m), 643 (w), 674 (m), 699 (m), 726 (w), 744 (w), 752 (w), 761 (w), 783 (w), 795 (m), 1024 (w), 1069 (w), 1135 (m), 1153 (m), 1177 (m), 1220 (w), 1230 (w), 1259 (w), 1290 (w), 1327 (w), 1376 (w), 1392 (w), 1416 (s), 1428 (vs), 1444 (m), 1454 (m), 1493 (w), 1560 (w), 1602 (w), 1636 (w), 1686 (w), 1733 (s), 2850 (w), 2872 (w), 2926 (w), 2959 cm<sup>-1</sup> (w).

[70]PCPB (50%): <sup>1</sup>H NMR (CS<sub>2</sub>/(CD<sub>3</sub>)<sub>2</sub>CO 9:1, 400 MHz): δ = 0.96 (t, 3H), 1.43 (m, 2H), 1.65 (m, 2H), 2.80 (m, 4H), 4.11 (t, 2H), 7.47 (t, 1H), 7.56 (t, 2H), 7.95 ppm (br d, 2H); <sup>13</sup>C NMR (CS<sub>2</sub>/(CD<sub>3</sub>)<sub>2</sub>CO 9:1, 150 MHz): δ = 14.42 (CH<sub>3</sub>), 20.00 (CH<sub>3</sub>CH<sub>2</sub>), 30.35, 31.08, 31.31, 35.30 (methane bridge C), 64.43 (O–CH<sub>2</sub>), 69.81 (cage sp<sup>3</sup> C), 71.86 (cage sp<sup>3</sup> C), 128.53, 128.82, 130.54, 130.74, 130.79, 130.95, 131.73, 132.83, 134.02, 136.75, 137.58, 137.79, 138.73, 139.49, 140.32, 141.15, 141.38, 141.65, 141.87, 142.64, 142.76, 143.37, 143.44, 143.73, 143.8, 143.97, 144.18, 144.64, 145.60, 145.75, 145.92, 146.02, 146.13, 146.35, 146.89, 147.03, 147.42, 147.48, 147.52, 147.56, 147.76, 147.93, 148.19, 148.39, 148.52, 148.56, 148.67,

149.13, 149.18, 149.25, 149.39, 149.45, 150.53, 150.58, 150.82, 150.85, 151.13, 151.19, 151.48, 151.99, 152.22, 155.25, 155.93, 170.74 ppm (COO); MALDI TOF MS:  $m/z=1058.11$  (calculated  $m/z=1058.13$ ); UV/Vis (toluene):  $\lambda=324, 357, 372, 402, 464, 537$  nm. FTIR (KBr):  $\nu=459$  (w), 534 (m), 578 (m), 644 (w), 674 (m), 699 (m), 727 (m), 795 (m), 1023 (w), 1030 (w), 1075 (w), 1135 (m), 1152 (m), 1177 (m), 1247 (w), 1297 (w), 1328 (w), 1372 (w), 1415 (s), 1428 (vs), 1443 (m), 1453 (m), 1494 (w), 1732 (s), 2852 (w), 2923 (w), 2944 (w), 2969  $\text{cm}^{-1}$  (w).

### Device fabrication and characterization

Organic solar cells were fabricated according to previously reported procedures.<sup>[16,31,38]</sup> A combination of lithium fluoride (0.6 nm) and aluminum (100 nm) was deposited in vacuum on MDMO-PPV/fullerene derivative blends. In the P3HT-based cells bare aluminum was used as cathode material. *I/V* characteristics of the devices were obtained in the dark and under the simulated 100  $\text{mWcm}^{-2}$  AM 1.5 solar irradiation provided by a KHS Steuernagel solar simulator. The intensity of the illumination was checked every time before the measurements using a calibrated silicon diode with known spectral response. All data given in this paper were not corrected for the mismatch between the solar simulator illumination and the AM 1.5 spectrum. The photocurrent spectra were measured with a SRS 830 lock-in amplifier using the monochromated light from a 75 W Xe lamp as excitation.

### Acknowledgements

Financial support was provided by the Russian Foundation for Basic Research (RFBR grant 10-03-00443a), Federal Agency for Science and Innovations (FASI contract 02.740.11.0749) and Russian President Foundation (grant MK-4305.2009.3).

- [1] F. G. Brunetti, R. Kumar, F. Wudl, *J. Mater. Chem.* **2010**, *20*, 2934–2948.
- [2] S. H. Park, A. Roy, S. Beaupre, S. Cho, N. Coates, J. S. Moon, D. Moses, M. Leclerc, K. Lee, A. J. Heeger, *Nat. Photonics* **2009**, *3*, 297–303.
- [3] Y. Liang, Z. Xu, J. Xia, S.-T. Tsai, Y. Wu, G. Li, C. Ray, L. Yu, *Adv. Mater.* **2010**, *22*, 1–4.
- [4] F. C. Krebs, *Sol. Energy Mater. Sol. Cells* **2009**, *93*, 465–475.
- [5] F. C. Krebs, M. Jorgensen, K. Norrman, O. Hagemann, J. Alstrup, T. D. Nielsen, J. Fyenbo, K. Larsen, J. Kristensen, *Sol. Energy Mater. Sol. Cells* **2010**, *93*, 422–441.
- [6] F. C. Krebs, S. A. Gevorgyan, J. Alstrup, *J. Mater. Chem.* **2009**, *19*, 5442–5451.
- [7] <http://www.konarkatech.com/>.
- [8] G. Dennler, M. C. Scharber, C. J. Brabec, *Adv. Mater.* **2009**, *21*, 1323–1338.
- [9] J. Chen, Y. Cao, *Acc. Chem. Res.* **2009**, *42*, 1709–1718.
- [10] H. Hoppe, N. S. Sariciftci in *Photoresponsive Polymers II Advances in Polymer Science* (Eds.: S. R. Marder, K.-S. Lee), Springer Berlin-Heidelberg, **2008**, pp. 1–86.
- [11] Y.-J. Cheng, S.-H. Yang, C.-S. Hsu, *Chem. Rev.* **2009**, *109*, 5868–5923.
- [12] L. M. Popescu, P. van't Hof, A. B. Sieval, H. T. Jonkman, J. C. Hummelen, *Appl. Phys. Lett.* **2006**, *89*, 213507.
- [13] M. Lenes, G.-J. A. H. Wetzelaer, F. B. Kooistra, S. C. Veenstra, J. C. Hummelen, P. W. M. Blom, *Adv. Mater.* **2008**, *20*, 2116–2119.
- [14] C. Yang, J. Y. Kim, S. Cho, J. K. Lee, A. J. Heeger, F. Wudl, *J. Am. Chem. Soc.* **2008**, *130*, 6444–6450.
- [15] R. B. Ross, C. M. Cardona, D. M. Guldi, S. G. Sankaranarayanan, M. O. Reese, N. Kipodakis, J. Peet, B. Walker, G. C. Bazan, E. Van Keuren, B. C. Holloway, M. Drees, *Nat. Mater.* **2009**, *8*, 208–212.
- [16] J. A. Renz, P. A. Troshin, G. Gobsch, V. F. Razumov, H. Hoppe, *Phys. Status Solidi RRL* **2008**, *2*(6), 263–265.
- [17] P. A. Troshin, H. Hoppe, J. Renz, M. Egginger, J. Yu. Mayorova, A. E. Goryachev, A. S. Peregudov, R. N. Lyubovskaya, G. Gobsch, N. S. Sariciftci, V. F. Razumov, *Adv. Funct. Mater.* **2009**, *19*, 779–788.
- [18] S. A. Backer, K. Sivula, D. F. Kavulak, J. M. J. Frechet, *Chem. Mater.* **2007**, *19*, 2927–2929.
- [19] P. A. Troshin, E. A. Khakina, M. Egginger, A. E. Goryachev, S. I. Troyanov, A. Fuchsbaue, A. S. Peregudov, R. N. Lyubovskaya, V. F. Razumov, N. S. Sariciftci, *ChemSusChem* **2010**, *3*, 356.
- [20] P. A. Troshin, R. Koeppel, D. K. Susarova, N. V. Polyakova, A. S. Peregudov, V. F. Razumov, N. S. Sariciftci, R. N. Lyubovskaya, *J. Mater. Chem.* **2009**, *19*, 7738–7744.
- [21] J. L. Delgado, P.-A. Bouit, S. Filippone, M. A. Herranz, N. Martin, *Chem. Commun.* **2010**, *46*, 4853–4865.
- [22] D. Mühlbacher, M. Scharber, M. Morana, Z. Zhu, D. Waller, R. Gaudiana, C. Brabec, *Adv. Mater.* **2006**, *18*, 2884–2889.
- [23] J. Peet, J. Y. Kim, N. E. Coates, W. L. Ma, D. Moses, A. J. Heeger, G. C. Bazan, *Nat. Mater.* **2007**, *6*, 497.
- [24] J. Hou, H.-Y. Chen, S. Zhang, G. Li, Y. Yang, *J. Am. Chem. Soc.* **2008**, *130*, 16144–16145.
- [25] Y. Liang, Y. Wu, D. Feng, S.-T. Tsai, H.-J. Son, G. Li, L. Yu, *J. Am. Chem. Soc.* **2009**, *131*, 56–57.
- [26] Y. Liang, Y. Wu, D. Feng, S.-T. Tsai, G. Li, C. Ray, L. Yu, *J. Am. Chem. Soc.* **2009**, *131*, 7792–7799.
- [27] [www.solennebv.com/](http://www.solennebv.com/); [www.adsdyes.com/fullerenes.html](http://www.adsdyes.com/fullerenes.html); <http://www.sesres.com/FullerenesPrices.asp>; <http://www.mercorp.com/mercorp/>; <http://www.mtr-ltd.com/>.
- [28] X. Wang, E. Perzon, J. L. Delgado, P. De La Cruz, F. Zhang, F. Langa, M. Andersson, O. Inganäs, *Appl. Phys. Lett.* **2004**, *85*, 5081–5083.
- [29] X. Wang, E. Perzon, F. Oswald, F. Langa, S. Admassie, M. R. Andersson, O. Inganäs, *Adv. Funct. Mater.* **2005**, *15*, 1665–1670.
- [30] J. L. Delgado, E. Espíldora, M. Liedtke, A. Sperlich, D. Rauh, A. Baumann, C. Deibel, V. Dyakonov, N. Martín, *Chem. Eur. J.* **2009**, *15*, 13474.
- [31] M. M. Wienk, J. M. Kroon, W. J. H. Verhees, J. Knol, J. C. Hummelen, P. A. van Hall, R. A. J. Janssen, *Angew. Chem.* **2003**, *115*, 3493–3497; *Angew. Chem. Int. Ed.* **2003**, *42*, 3371–3375.
- [32] J. C. Hummelen, B. W. Knight, F. Lepeq, F. Wudl, J. Yao, C. L. Wilkins, *J. Org. Chem.* **1995**, *60*, 532.
- [33] K. Maturova, S. S. van Bavel, M. M. Wienk, R. A. J. Janssen, M. Kemerink, *Nano Lett.* **2009**, *9*, 3032–3037.
- [34] H. J. Bolink, E. Coronado, A. Forment-Aliaga, M. Lenes, A. La Rosa, S. Filippone, N. Martin, *J. Mater. Chem.* **2010** DOI: 10.1039/c0jm01160f.
- [35] A. Sánchez-Díaz, M. Izquierdo, S. Filippone, N. Martín, E. Palomares, *Adv. Funct. Mater.* **2010**, *20*, 2695–2700.
- [36] H. Hoppe, N. Arnold, D. Meissner, N. S. Sariciftci, *Sol. Energy Mater. Sol. Cells* **2003**, *80*, 105–113.
- [37] H. Hoppe, N. Arnold, D. Meissner, N. S. Sariciftci, *Thin Solid Films* **2004**, *451–452*, 589–592.
- [38] H. Hoppe, S. Shokhovets, G. Gobsch, *Phys. Status Solidi RRL* **2007**, *1*, R40–R42.
- [39] S. E. Shaheen, C. J. Brabec, N. S. Sariciftci, F. Padinger, T. Fromherz, J. C. Hummelen, *Appl. Phys. Lett.* **2001**, *78*, 841–843.

Received: August 5, 2010

Revised: September 14, 2010

Published online on December 23, 2010